Archives of Biochemistry and Biophysics 700 (2021) 108755

Contents lists available at ScienceDirect

Archives of Biochemistry and Biophysics

journal homepage: www.elsevier.com/locate/yabbi

Characterization of aldo-keto reductase 1C subfamily members encoded in two rat genes (*akr1c19* and *RGD1564865*). Relationship to 9-hydroxyprostaglandin dehydrogenase

Satoshi Endo [a,*], Toshiyuki Matsunaga [b], Akira Hara [c]

[a] Laboratory of Biochemistry, Gifu Pharmaceutical University, Gifu, 501-1196, Japan
[b] Education Center of Green Pharmaceutical Sciences, Gifu Pharmaceutical University, Gifu, 502-8585, Japan
[c] Faculty of Engineering, Gifu University, Gifu, 501-1193, Japan

ARTICLE INFO

Keywords:
9-hydroxyprostaglandin dehydrogenase
Aldo-keto reductase
$PGF_{2\alpha}$
9α,11β-PGF_2
PGD_2

ABSTRACT

Rat genes, *akr1c19* and *RGD1564865*, encode members (R1C19 and 20HSDL, respectively) of the aldo-keto reductase (AKR) 1C subfamily, whose functions, however, remain unknown. Here, we show that recombinant R1C19 and 20HSDL exhibit NAD^+-dependent dehydrogenase activity for prostaglandins (PGs) with 9α-hydroxy group ($PGF_{2\alpha}$, its 13,14-dihydro- and 15-keto derivatives, 9α,11β-PGF_2 and PGD_2). 20HSDL oxidized the PGs with much lower K_m (0.3–14 μM) and higher k_{cat}/K_m values (0.064–2.6 $min^{-1}\mu M^{-1}$) than those of R1C19. They also differed in other properties: R1C19, but not 20HSDL, oxidized some 17β-hydroxysteroids (5β-androstane-3α,17β-diol and 5β-androstan-17β-ol-3-one). 20HSDL was specifically inhibited by zomepirac, but not by R1C19-selective inhibitors (hexestrol, flavonoids, ibuprofen and flufenamic acid), although the two enzymes were sensitive to indomethacin and *cis*-unsaturated fatty acids. The mRNA for 20HSDL was expressed abundantly in rat kidney and at low levels in the liver, testis, brain, heart and colon, in contrast to ubiquitous expression of R1C19 mRNA. The comparison of enzymic features of R1C19 and 20HSDL with rat PG dehydrogenases and other AKRs suggests not only a close relationship of 20HSDL with 9-hydroxy-PG dehydrogenase in rat kidney, but also roles of R1C19 and rat AKRs (1C16 and 1C24) in the metabolism of $PGF_{2\alpha}$, PGD_2 and 9α,11β-PGF_2 in other tissues.

1. Introduction

The aldo-keto reductase (AKR) superfamily is a rapidly growing group of NAD(P)(H)-dependent oxidoreductases that metabolize carbohydrates, steroids, prostaglandins, and other endogenous aldehydes and ketones, as well as xenobiotic compounds [1,2], (https://www.med.upenn.edu/akr/). Currently there are more than 190 known members of this superfamily classified into 16 families. The largest family, AKR1, includes mammalian enzymes, which are subdivided into five subfamilies composed of enzymes in parentheses: AKR1A (aldehyde reductases); AKR1B (aldose reductases); AKR1C (hydroxysteroid dehydrogenases, HSDs); AKR1D (steroid-5β-reductases); and AKR1E (1, 5-anhydro-D-fuructose reductases), based on a >60% amino acid sequence identity (ASI). Among the five AKR1 subfamilies, the number of members belonging to the AKR1C subfamily is different depending on mammalian species. Human AKR1C subfamily members (AKR1Cs) are four NADPH-dependent HSDs: AKR1C1 (20α-HSD), AKR1C2 (type-3 3α-HSD), AKR1C3 (type-2 3α-HSD/type-5 17β-HSD) and AKR1C4 (type-1 3α-HSD) [2,3]. The four enzymes also reduce endogenous and xenobiotic nonsteroidal carbonyl compounds, and act as drug metabolizing enzymes [4]. In a laboratory animal mouse, AKR1Cs are nine, which include not only five NADPH-dependent HSDs and prostaglandin (PG)D_2 11-ketoreductase [5–11], but also NAD^+-preferring enzymes that show dehydrogenase activities towards hydroxysteroids (AKR1C12 and AKR1C13) and alicyclic alcohols (AKR1C19) [12–14], as shown in Table 1. In another laboratory animal rat, ten AKR1Cs are annotated in

Abbreviations: AKR, aldo-keto reductase; AKR1Cs, AKR1C subfamily members; ASI, amino acid sequence identity; 9HPD, 9-hydroxyprostaglandin dehydrogenase; HSD, hydroxysteroid dehydrogenase; 20HSDL, rat 20α-hydroxysteroid dehydrogenase-like; NSAID, nonsteroidal anti-inflammatory drug; PG, prostaglandin; R1C19, rat AKR1C19; RT, reverse transcription.

* Corresponding author.
E-mail address: sendo@gifu-pu.ac.jp (Satoshi Endo).

https://doi.org/10.1016/j.abb.2021.108755
Received 23 October 2020; Received in revised form 5 January 2021; Accepted 7 January 2021
Available online 19 January 2021

the NCBI gene database (https://www.ncbi.nlm.nih.gov/gene). Among them, eight members (HSD17B5, AKR1C9, AKR1C8, RAKg, AKR1C15, AKR1C24, AKR1C16 and AKR1C17) are enzymatically characterized [4,13,15–20], and two (AKR1C15 and AKR1C17) of them are rat-unique enzymes that structurally and functionally differ from human and mouse AKR1Cs. Other two rat AKR1Cs encoded in the *akr1c19* and *RGD1564865* genes are currently annotated as rat AKR1C19 and rat 20α-HSD-like (here designated as R1C19 and 20HSDL, respectively), but their enzymatic properties remain unknown.

R1C19 of the uncharacterized rat AKR1Cs is most homologous (92% ASI) to mouse AKR1C19. Mouse AKR1C19 is a ubiquitously expressed NAD(H)-preferring enzyme that oxidizes some alicyclic alcohols and reduces α-dicarbonyl compounds, but its endogenous substrate is unknown [14]. Another uncharacterized rat AKR1C, 20HSDL, has less ASI (61%–70%) to human and mouse AKR1Cs and other rat AKR1Cs. The mRNA for 20HSDL is noted to be biasedly expressed in adult rat kidney, liver and testis in the NCBI gene database. Although the function of 20HSDL is unknown, its renal expression is decreased in a rat model of polycystic kidney disease [21], and its hepatic expression is upregulated by administration of a thyroid disruptor, fipronil [22]. In order to elucidate the functions of R1C19 and 20HSDL, we have here prepared their recombinant proteins and examined their enzymatic properties and tissue expression. Since the two enzymes exhibited 9-hydroxyprostaglandin dehydrogenase (9HPD) activity, PG specificity of other rat NAD^+-preferring AKR1Cs (1C16, 1C17 and 1C24) and mouse AKR1C19 was also studied.

2. Materials and methods

2.1. Materials

PGs were obtained from Santa Cruz Biotechnology (Dallas, TX, USA), Cayman Chemical (Ann Arbor, MI, USA) and Ono Pharmaceutical Co (Osaka, Japan); and steroids were obtained from Sigma Chemicals (Perth, WA, USA) and Steraloids (Newport, RI, USA). *trans*-Benzene dihydrodiol (*trans*-1,2-dihydrobenzene-1,2-diol) was synthesized as described previously [23]. 3β-Hydroxyhexobarbital was gifted from Dr. R. Takenoshita (University of Fukuoka, Japan). pcDNA3.1+/C-(K)DYK plasmids harboring the cDNA for 20HSDL were purchased from Genscript Biotech Co (Piscataway, NJ, USA). pCold I expression vectors were obtained from Takara (Kusatsu, Japan); restriction enzymes were from Invitrogen (Carlsbad, CA, USA); and KOD FX neo DNA polymerase and Quick Taq HS DyeMix were from TOYOBO (Osaka, Japan). All other chemicals were of the highest grade that could be obtained commercially.

2.2. Production of recombinant enzymes

To express the recombinant 20HSDL in *Escherichia coli* systems, its cDNA was amplified from the pcDNA3.1+/C-(K)DYK plasmids by PCR using the KOD FX neo DNA polymerase and a pair of sense and antisense primers, which contain *Nde*I and *Sal*I sites. The primer sequences and PCR conditions are shown in Table S1 (Supplementary Data). The PCR products were purified, and ligated into the pCold I vectors that had been digested with the two restriction enzymes (New England Biolabs, Ipswich, MA). The insert of the cloned cDNA was sequenced by using an ABI Prism 3130 Genetic Analyzer (Thermo Fisher Scientific, Waltham, MA, USA), to confirm that the nucleotide sequence (accession no. NM_001164396.1) of 20HSDL fused to that for the N-terminal 6-H-tag is encoded.

The cDNA for R1C19 was amplified by reverse transcription (RT)-PCR from total RNA of a 40-weeks-old female Wistar rat liver. The preparation of the total RNA and RT were carried out as described previously [24]. PCR was performed with the KOD FX neo DNA polymerase and primers, whose sequences and PCR conditions are shown in Supplementary Table S1. The PCR products were ligated into the pCold I vectors, and the insert of the cloned cDNA was sequenced as described above. The sequence of the cDNA differed by two nucleotides (^{48}T→C and ^{794}A→T) from that predicted from rat *akr1c19* gene (accession no. NM_001100576.1), and was deposited in the DDBJ database with the accession no. LC579561.

The constructed expression plasmids were transformed into *E. coli* BL21 (DE3) pLysS cells (Life Technologies, Carlsbad, CA). The recombinant enzymes were expressed and purified from the cell extract using a Ni Sepharose 6 Fast Flow resin (GE healthcare, Little Chalfont, UK) according to the manufacturer's manual. The representative yields of the homogeneous 20HSDL and R1C19 were 9 and 21 mg, respectively, per 2-L *E. coli* culture. Protein concentration was determined by Bradford's method using bovine serum albumin as the standard [25]. Recombinant AKR1C16 [13], AKR1C17 [20], AKR1C24 [15] and mouse AKR1C19 [14] were expressed in *E. coli* cells transformed with the expression plasmids harboring their cDNAs, and were purified as previously

Table 1
Mouse and rat AKR1C subfamily members.

Mouse Gene[a]	Protein[b]	Enzymatic activity[c]	Ref.	Rat Gene[a]	Protein[b]	Enzymatic activity[c]	ASI[d] %	Ref.
NADPH-dependent enzyme				NADPH-dependent enzyme				
Akr1c6	AKR1C6	17β-HSD, CR	[5]	*Akr1c1*	(HSD17B5)	17β/20α-HSD, CR	86	[15]
Akr1c14	AKR1C14	3α-HSD, CR	[6,7]	*Akr1c14*	AKR1C9	3α-HSD, CR	87	[16,17]
Akr1c18	AKR1C18	20α-HSD, CR	[8]	*Akr1c3*	AKR1C8	20α-HSD, CR	93	[18]
Akr1c21	AKR1C21	3(17)α-HSD, CR	[9]	*Akr1c2*	(RAKg)	3(17)α-HSD, CR	87	[4]
Akr1c20	AKR1C20[e]	3α/17β-HSD, CR	[10]	*Akr1c15*	AKR1C15[f]	17β-HSD, CR		[19]
Akr1cl	(AKR1CL)[e]	PGD_2 11-ketoreductase	[11]					
NAD^+-preferring enzyme				NAD^+-preferring enzyme				
Akr1c12	AKR1C12	3α/17β/20α-HSD, ADH	[12]	*Akr1c12*	AKR1C24	3α/17β/20α-HSD, ADH	91	[15]
Akr1c13	AKR1C13	3α/17β/20α-HSD, ADH	[13]	*Akr1c13*	AKR1C16	3α/17β/20α-HSD, ADH	93	[13]
Akr1c19	AKR1c19	ADH	[14]	*Akr1c19*	(R1C19)	17β-HSD, 9HPD, ADH	92	This study
				Akr1c12l1	AKR1C17[f]	3α-HSD		[20]
				RGD1564865	(20HSDL)[f]	9-HPD, ADH		This study

[a] Gene name annotated in the NCBI gene database. Rat gene names may not infer homology across species.
[b] Protein name assigned in the AKR superfamily homepage (https://www.med.upenn.edu/akr/), except that those in parentheses are taken from their references.
[c] Abbreviations: HSD, hydroxysteroid dehydrogenase; CR, reductase toward xenobiotic carbonyl compounds; ADH, dehydrogenase towards xenobiotic alicyclic alcohols; and 9HPD, 9-hydroxyprostaglandin dehydrogenase.
[d] The amino acid sequence identity (ASI) % with the mouse enzyme shown on the left in the same row. This is also the highest on alignment analysis against all the mouse enzymes.
[e] Mouse-specific proteins that do not show identical enzymatic activity and/or >70% ASI with the rat enzymes.
[f] Rat-specific proteins that do not show identical enzymatic activity and/or >70% ASI with the mouse enzymes.

described. The purified enzymes showed single bands on SDS-PAGE analysis (Supplementary Fig. S1).

2.3. Assay of enzyme activity

Reductase and dehydrogenase activities were assayed by measuring the rate of change in NAD(P)H absorbance (at 340 nm) and its fluorescence emission (at 455 nm with an excitation wavelength of 340 nm), respectively, in a 1-mL reaction mixture containing 0.1 M potassium phosphate (pH 7.0), 0.1 mM NADH or 1 mM $NAD(P)^+$, substrate and enzyme [13]. The substrate concentrations were 0.1–200 μM (for PGs), 10–100 μM (for steroids), 1–25 mM (for monosaccharides) and 0.1–2 mM (for other carbonyls and alcohols). One unit (U) of enzyme activity was defined as the enzyme amount that catalyzes the oxidation or formation of 1 μmol of NAD(P)H per min at 25 °C. The K_m and V_{max} values were determined over a range of five substrate concentrations by fitting Michaelis-Menten equation and/or Lineweaver-Burk plot analysis of the initial velocities using the program Hyper 32 (University of Liverpool, UK). The enzyme concentrations used in the kinetic studies were 2–10 μg/mL (for R1C19, AKR1C16, AKR1C17 and AKR1C19) and 0.8–4 μg/mL (for 20HSDL and AKR1C24). k_{cat} value was calculated from the V_{max} value based on molecular weights of His-tagged R1C19 (38,959), His-tagged 20HSDL (39,047), and AKR1C19 (37,046). The IC_{50} values for inhibitors were determined in the NAD^+-linked oxidation of 2 μM PGD_2 (for 20HSDL, 0.8 μg/mL) and 25 μM β-ionol (for R1C19, 2 μg/mL). The kinetic constants are expressed as the means ± SE of at least three determinations.

2.4. Product identification

The reaction was conducted in a 2-mL reaction mixture, containing 1 mM NAD^+, PG, enzyme (25–50 μg) and 0.1 M potassium phosphate, pH 7.4. The substrate concentrations and incubation times were 25 μM and 15 min, respectively, for the oxidation of PGD_2 and 13,14-dihydro-15-keto-$PGF_{2\alpha}$, and were 50 μM and 30 min, respectively, for that of other PGs. The reaction was stopped by adding 1 M Na_2SO_4 (0.5 mL) and diethyl ether/methanol/citric acid (30:4:1, v/v; 2 mL), and the substrate and product were extracted into the ether. After the ether phase was dried under vacuum, the residue was dissolved in methanol and analyzed by thin-layer chromatography using silica-gel plates in a solvent system of ethyl acetate/methylene chloride/acetone/methanol/acetic acid (90:30:10:8:1, v/v) [26]. The PGs and authentic samples (13, 14-dihydro-15-keto-$PGF_{2\alpha}$, 13,14-dihydro-15-keto-PGE_2, PGD_2, PGK_2, $PGF_{2\alpha}$, PGE_2, 9α,11β-PGF_2,11β-PGE_2) were visualized with iodine vapor.

2.5. Determination of K_d value for coenzyme

The K_d values for $NAD(P)^+$ to R1C19 and 20HSDL were determined by measuring intrinsic tryptophan fluorescence (at 334 nm with an excitation wavelength of 290 nm) of 1.0 μM enzyme in 0.1 M potassium phosphate, pH 7.4, at 25 °C, as described previously [27]. The K_d value is expressed as the mean ± SE of three determinations.

2.6. RT-PCR

Total RNAs of the female Wistar rat tissues and a male rat testis were prepared, and subjected to RT-PCR as described above. PCR was performed using the Quick Taq HS DyeMix and primers for R1C19, 20HSDL and β-actin (as an internal control), which are shown in Table S1 (Supplementary data). The PCR products were separated by agarose gel electrophoresis, and revealed with ethidium bromide.

3. Results and discussion

3.1. Coenzyme and substrate specificity

The amino acid sequence deduced from the isolated cDNA for R1C19 (Fig. 1) was identical to that predicted from its gene (*akr1c19*), except that the residue at position 265 is Ile instead of Asn in the predicted sequence. R1C19 showed the highest ASI (92%) to mouse AKR1C19 [14] among members of the AKR superfamily, whereas 20HSDL shared low ASI (61–69%) with mouse and other rat AKR1Cs listed in Table 1. Crystallographic and site-directed mutagenesis studies of AKR1Cs have shown that the residues at positions 270 and 276 are critical for coenzyme specificity: Those are Lys270 and Arg276 for the preference for NADP(H), and are Gln270 and Glu276 for the NAD(H) specificity [2,20]. Gln270 and Glu276 are conserved not only in NAD^+-preferring mouse AKR1C19, but also in R1C19 and 20HSDL. Since R1C19 and 20HSDL are, thus, expected to exhibit coenzyme specificity for NAD(H), we purified the two recombinant 39-kDa monomeric enzymes and tested their NAD^+-linked dehydrogenase activities towards hydroxysteroids and xenobiotic alcohols that are substrates of other rat AKR1Cs [13,15–20] and mouse AKR1C19 [14].

R1C19 oxidized three 17β-hydroxysteroids and β-ionol, in addition to (*S*)-1-indanol, 3β-hydroxyhexobarbital and *cis*-benzene dihydrodiol that are reported as the substrates of mouse AKR1C19 [14] (Table 2). Among the substrates, 5β-androstane-3α,17β-diol and β-ionol were the most efficient substrates, showing high k_{cat}/K_m values. By contrast, most of the R1C19 substrates were not oxidized by 20HSDL, which instead exhibited dehydrogenase activities towards *trans*-benzene dihydrodiol and (1*S*,2*S*)-*trans*-1,2-cyclohexanediol. Neither R1C19 nor 20HSDL oxidized other xenobiotic alcohols and hydroxysteroids (listed in Table 2), most of which are substrates of other rat AKR1Cs [13,15–20]. It should be noted that 20HSDL does not accept 20α-hydroxysteroids as its substrates, contrary to the current protein name encoded in the *RGD1564865* gene.

Intriguingly, both R1C19 and 20HSDL oxidized seven 9α-hydroxy-PGs, of which 13,14-dihydro-15-keto-$PGF_{2\alpha}$ was the most efficient substrate showing the highest k_{cat}/K_m value, followed by 15-keto-$PGF_{2\alpha}$ and PGD_2 (Table 2 and Supplementary Fig. S3). Such activity has not been reported for other rodent AKR1Cs as shown in Table 1. R1C19 and 20HSDL showed a similar reactivity towards changes in the two hydrocarbon chains of PG: 13,14-Dihydro- and 15-keto-derivatives were oxidized more efficiently than $PGF_{2\alpha}$, whereas the hydrogenation of the C5=C6 double bond on the opposite hydrocarbon chain (13,14-dihydro-15-keto-$PGF_{1\alpha}$ and PGD_1) markedly decreased the catalytic efficiency compared to the corresponding PGs with this double bond (13,14-dihydro-15-keto-$PGF_{2\alpha}$ and PGD_2, respectively). In addition to the structure of the hydrocarbon chains, the substituent on the five-membered ring may affect the catalytic efficiency of the enzymes, because PGD_2 with 11-keto group was more efficiently oxidized than $PGF_{2\alpha}$ and 9α,11β-PGF_2 with 11α- or 11β-hydroxy group. No activity was observed towards PGs without 9α-hydroxy group ($PGF_{2\beta}$, PGE_2, 11β-PGE_2, 13,14-dihydro-15-keto-PGE_2, PGI_2, PGA_2, PGA_1, PGB_2 and PGB_1). The substrate specificity indicates that the two enzymes catalyze the oxidation of the 9α-hydroxy-PGs into their 9-keto metabolites. Indeed, the oxidized products of 13,14-dihydro-15-keto-$PGF_{2\alpha}$, $PGF_{2\alpha}$ and 9α,11β-PGF_2 by 20HSDL were identified with 13,14-dihydro-15-keto-PGE_2, PGE_2 and 11β-PGE_2, respectively, on thin-layer chromatography analysis (Fig. 2). In the oxidation of PGD_2, the substrate amount was decreased compared to the no-incubation blank, but a very small amount of the reaction product with a R_f similar to authentic PGK_2 was formed. This might result from the instability of the assumed 9-keto product, PGK_2, because PGK_2 could not be detected in the analysis of the extract of a reaction mixture containing PGK_2, instead of PGD_2.

For R1C19, the k_{cat}/K_m values for 13,14-dihydro-15-keto-$PGF_{2\alpha}$ and 15-keto-$PGF_{2\alpha}$ were higher than those for the xenobiotic and steroidal substrates (β-ionol and 5β-androstane-3α,17β-diol, respectively),

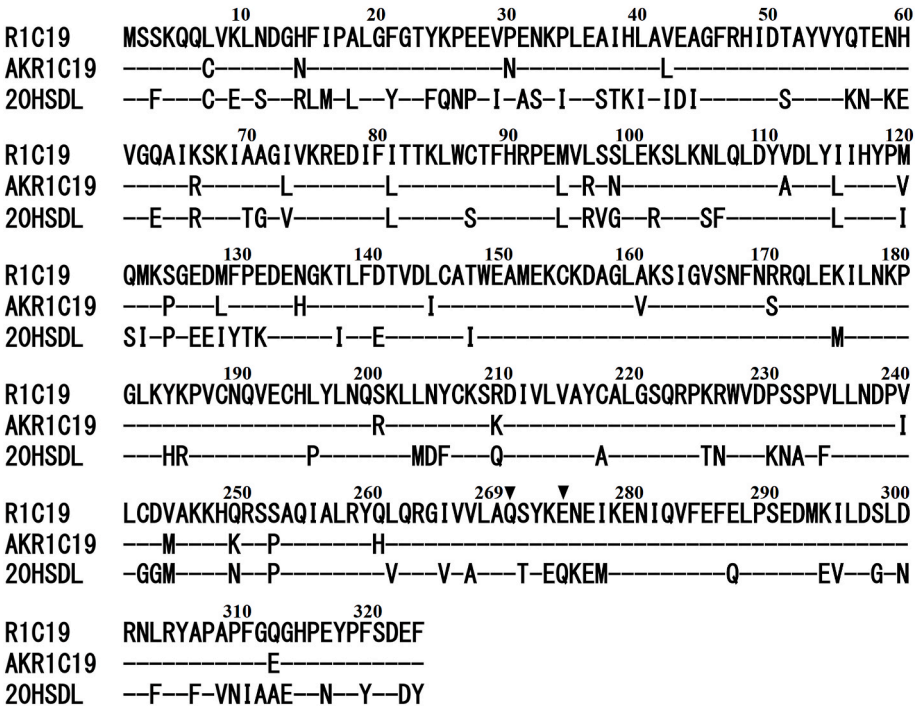

Fig. 1. Alignment of amino acid sequences of R1C19, mouse AKR1C19 (AKR1C19) and 20HSDL. The hyphens in the AKR1C19 and 20HSDL sequences represent identical residues to those of R1C19. The residues involved in NAD(H) preference of other AKR1Cs are indicated with closed arrowheads.

Table 2
Substrate specificity in NAD^+-linked oxidation.

Substrate	R1C19 K_m (μM)	k_{cat} (min^{-1})	k_{cat}/K_m (min^{-1} mM^{-1})	20HSDL K_m (μM)	k_{cat} (min^{-1})	k_{cat}/K_m (min^{-1} mM^{-1})
[Xenobiotic alcohols]						
β-Ionol	25 ± 2	0.48 ± 0.06	19		ns[a]	
3β-Hydroxyhexobarbital	100 ± 8	0.21 ± 0.03	2.1		ns	
(*S*)-1-Indanol	350 ± 22	0.52 ± 0.06	1.5		0.06[b]	
cis-Benzene dihydrodiol	2100 ± 320	1.2 ± 0.2	0.57	3500 ± 300	0.86 ± 0.19	0.25
trans-Benzene dihydrodiol		ns[a]		216 ± 20	0.62 ± 0.04	0.29
(1*S*,2*S*)-*trans*-1,2-Cyclohexanediol		ns[a]		980 ± 35	0.59 ± 0.02	0.60
Other alcohols[c]		ns[a]			ns[a]	
[Hydroxysteroids]						
5β-Androstane-3α,17β-diol	34 ± 2	0.49 ± 0.02	14		ns[a]	
5β-Androstan-17β-ol-3-one	77 ± 18	0.49 ± 0.06	6.4		ns[a]	
Testosterone	77 ± 8	0.12 ± 0.01	1.6		ns[a]	
Other hydroxysteroids[d]		ns[a]			ns[a]	
[PGs]						
13,14-Dihydro-15-keto-$PGF_{2\alpha}$	35 ± 3	1.6 ± 0.2	46	0.31 ± 0.05	0.82 ± 0.08	2600
15-Keto-$PGF_{2\alpha}$	18 ± 1	0.39 ± 0.02	22	2.6 ± 0.2	0.98 ± 0.08	380
PGD_2	12 ± 1	0.086 ± 0.012	7.2	1.8 ± 0.2	1.5 ± 0.1	830
9α,11β-PGF_2	264 ± 25	0.17 ± 0.03	0.64	14 ± 2	1.1 ± 0.2	79
$PGF_{2\alpha}$	215 ± 15	0.14 ± 0.02	0.65	9.2 ± 0.6	0.59 ± 0.04	64
PGD_1	106 ± 5	0.071 ± 0.011	0.67	27 ± 3	0.51 ± 0.04	19
13,14-Dihydro-15-keto-$PGF_{1\alpha}$	93 ± 15	0.045 ± 0.003	0.48	8.6 ± 1.2	0.62 ± 0.04	73
Other PGs[e]		ns[a]			ns[a]	

Structures of substrates and their predicted products are shown in Supplementary Fig. S2.

[a] ns: no significant activity was observed.

[b] Calculated from the specific activity with 1 mM substrate.

[c] (*R*)-1-Indanol, (1*R*,2*R*)-*trans*-1,2-cyclohexanediol, 1-nonanol, geraniol, farnesol, sorbitol, xylitol, pyridine-4-methanol, and benzyl alcohol.

[d] 5α-Androstane-3α,17β-diol, 5α/β-androstane-3β,17β-diols, 5α-androstan-17β-ol-3-one, 5α/β-androstan-3α/β-ol-17-ones, epitestosterone, 17α/β-estradiols, 3α/β-hydroxyprogesterones, 20α/β-hydroxyprogesterones, 5α/β-pregnane-3α,20α-diols, deoxycoticosterone and cortisol.

[e] $PGF_{2\beta}$ (9β,11α-PGF_2), PGE_2, 11β-PGE_2, 13,14-dihydro-15-keto-PGE_2, PGI_2, PGA_2, PGA_1, PGB_2 and PGB_1.

suggesting that the enzyme is involved in the metabolism of the two PGs. 20HSDL oxidized all the PG substrates more efficiently than R1C19 due to its much lower K_m values, and its k_{cat}/K_m values for the PGs were greatly higher than those for the above xenobiotic alcohol substrates. Thus, 20HSDL may act as an efficient 9HPD, especially towards 13,14-dihydro-15-keto-$PGF_{2\alpha}$ and PGD_2.

In the NADH-linked reverse reaction, R1C19 reduced several α-dicarbonyl compounds, of which the alicyclic and aromatic substrates (camphorquinones and isatin) were reduced more efficiently than the aliphatic ones (Table 3). R1C19 did not exhibit significant activities for

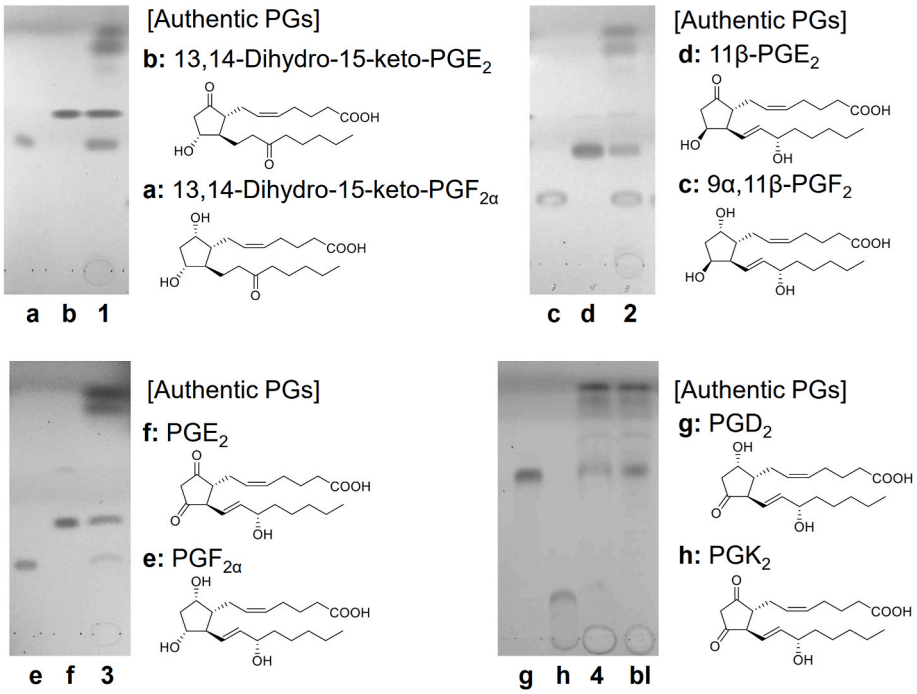

Fig. 2. Thin-layer chromatograms of the products in the oxidation of 13,14-dihydro-15-keto-$PGF_{2\alpha}$ (1), 9α,11β-PGF_2 (2), $PGF_{2\alpha}$ (3), and PGD_2 (4) by 20HSDL. Blank without incubation (bl) was included in the analysis of PGD_2 oxidation product. Authentic PGs (a–h) and their structures are shown in the right. Spots with high Rf values are unknown.

Table 3
Substrate specificity in NADH-linked reduction.

Substrate	R1C19 K_m (μM)	k_{cat} (min^{-1})	k_{cat}/K_m (min^{-1} mM^{-1})	20HSDL K_m (μM)	k_{cat} (min^{-1})	k_{cat}/K_m (min^{-1} mM^{-1})
(1*S*)-Camphorquinone	2.6 ± 0.4	4.8 ± 0.2	1846	2.6 ± 0.2	0.39 ± 0.004	150
Isatin	3.6 ± 0.4	3.2 ± 0.2	889		ns[a]	
(1*R*)-Camphorquinone	3.6 ± 0.3	2.1 ± 0.2	583	20 ± 3	0.26 ± 0.03	13
2,3-Heptanedione	27 ± 3	1.2 ± 0.1	44		0.14[b]	
2,3-Pentanedione	115 ± 3	1.6 ± 0.2	14	113 ± 8	0.36 ± 0.04	3.2
2,3-Hexanedione	84 ± 12	1.1 ± 0.1	13	172 ± 8	0.38 ± 0.03	2.2
Diacetyl	1400 ± 150	2.5 ± 0.1	1.8	470 ± 50	0.39 ± 0.04	0.83
13,14-Dihydro-15-keto-PGE_2		ns[a]		2.0 ± 0.5	0.070 ± 0.008	35
Other carbonyls[c]		ns[a]			ns[a]	

Structures of substrates are shown in Supplementary Fig. S4.
[a] ns: no significant activity was detected.
[b] Calculated from the specific activity with 0.1 mM substrate.
[c] Steroids (5β-androstan-3α/β-ol-17-ones, 5β-androstane-3,17-dione and 4-androstene-3,17-dione), PGs (13,14-dihydro-15-keto-$PGF_{1\alpha}$, PGK_2, PGE_2 and 11β-PGE_2), *p*-quinones (menadione and 1,4-naphthoquinone), xenobiotic ketones (4-benzoylpyridine and 4-nitroacetophenone), and aldehydes (pyridine-3/4-aldehydes).

17-ketosteroids and 9-keto-PGs, suggesting that its oxidation of 9α-hydroxy-PGs and 17β-hydroxysteroids is apparently irreversible. Similar substrate specificity for the carbonyl compounds was observed for 20HSDL, but its k_{cat} and k_{cat}/K_m values were lower than those of R1C19. In addition, 20HSDL reduced 13,14-dihydro-15-keto-PGE_2, although its k_{cat}/K_m value was much lower than that for corresponding alcohol substrate 13,14-dihydro-15-keto-$PGF_{2\alpha}$ in the oxidation. The two enzymes did not reduce *p*-quinones, xenobiotic ketones, and aldehydes (listed in Table 3), which are substrates of known rodent AKR1Cs other than mouse AKR1C19 [14] and AKR1CL [11]. With respect to the substrate specificity for α-dicarbonyl compounds, R1C19 is also similar to mouse AKR1C19 [14].

R1C19 exhibited dual coenzyme specificity for NAD^+ and $NADP^+$, but NAD^+ was the preferable coenzyme, giving lower K_m (1.8 ± 0.3 μM) for NAD^+ and higher k_{cat} (0.48 ± 0.06 min^{-1}) than those (23 ± 5 μM and 0.26 ± 0.05 min^{-1}, respectively) for $NADP^+$ in the 0.1-mM β-ionol oxidation. In contrast, 20HSDL was apparently NAD^+-dependent: In the 25-μM PGD_2 oxidation, its K_m value for NAD^+ was 34 ± 1 μM, but 1-mM $NADP^+$-linked activity was low (6% of the NAD^+-linked activity) and K_m value for $NADP^+$ could not be determined. The coenzyme preference was also evident from the K_d values for NAD^+ and $NADP^+$, which were 0.73 ± 0.08 and 22 ± 2 μM (for R1C19), and were 1.7 ± 0.2 and 33 ± 7 μM (for 20HSDL). The preference for NAD^+ over $NADP^+$ is probably determined by Gln270 and Glu276 in R1C19 and 20HSDL as described above. The concentration of NAD^+ in the cytoplasm of rat liver greatly exceeds that of NADH (1000:1), while the concentration of NADPH exceeds that of $NADP^+$ (1:100) [28]. Thus, both R1C19 and 20HSDL usually function in the oxidative direction in intact cells. The substrate specificity (Tables 2 and 3) also indicates that the enzymes solely act as dehydrogenases in the metabolism of PGs and/or steroids.

3.2. Inhibitor sensitivity

To further characterize R1C19 and 20HSDL, we examined effects of

inhibitors of the other rodent AKR1Cs on their dehydrogenase activities (Table 4). Such inhibitors of the rodent AKR1Cs are a synthetic estrogen, hexestrol [6,9,10,12,13,15,18], two flavonoids (genistein and quercitrin) [6,11–15,18,20,29], and nonsteroidal anti-inflammatory drugs (NSAIDs) [6,10,11,18,21]. Hexestrol and the two flavonoids inhibited R1C19, but not 20HSDL. R1C19 was more potently inhibited by other flavonoids, of which chrysin, the simplest flavone (Supplementary Fig. S5), was most potent. In contrast, the insensitivity of 20HSDL to hexestrol and flavonoids differs from properties of the above rodent AKR1Cs, and may be useful for discriminating this enzyme from rat NAD^+-preferring R1C19, AKR1C16 and AKR1C24 that exhibit 9HPD activity as described later.

R1C19 and 20HSDL also showed some differences in the sensitivity to NSAIDs. Although indomethacin inhibited both enzymes, ibuprofen, flufenamic acid and loxoprofen were inhibitory only to R1C19, and zomepirac was selectively inhibited 20HSDL. By contrast, the two enzymes were not inhibited by other NSAIDs listed in the footnote of Table 4. Such NSAID structure-dependent inhibition of the two enzymes is different from that of AKR1C9 [17], which is inhibited by many NSAIDs. In addition, R1C19 and 20HSDL were not inhibited by glycyrrhetinic acid, ethacrynic acid and medroxyprogesterone acetate, which are inhibitors of AKR1C17 [20], AKR1CL [11] and/or four rodent AKR1Cs [6,10,17,20].

Since unsaturated fatty acids have been reported to inhibit several PG-metabolizing enzymes [30–34], their effects on the dehydrogenase activities of R1C19 and 20HSDL were examined. The two enzymes were potently inhibited by *cis*-unsaturated fatty acids, in which numbers and/or location of the double bond and alkenyl chain length affected the inhibition potency to R1C19, but not that to 20HSDL. In contrast, the two enzymes were not inhibited by a *trans*-form of oleic acid (elaidic acid), methyl ester of linoleic acid (methyl linoleate) and their alcohol derivatives (oleyl and linoleyl alcohols). The structure-activity relationship suggests that the carboxylate end group of the *cis*-unsaturated fatty acids is essential for inhibition of both R1C19 and 20HSDL. The IC_{50} values for arachidonic acid, linoleic acid and/or oleic acid are comparable with IC_{50} or K_i values of rat 9HPD [30], PGD synthase [31], human PGF synthase (AKR1C3) [32] and NADPH-dependent PG 9-ketoreductase (carbonyl reductase 1) [33], inferring that endogenous *cis*-unsaturated fatty acids affect the metabolism mediated by R1C19 and 20HSDL.

Table 4
Inhibitor sensitivity of R1C19 and 20HSDL.

Inhibitor[a]	IC_{50} (μM)[b]	
	R1C19	20HSDL
[Synthetic estrogen]		
Hexestrol	9.4 ± 0.2	>20
[Flavonoids]		
Chrysin	0.15 ± 0.01	>20
Luteolin	2.0 ± 0.2	>20
Naringenin	4.4 ± 0.4	>20
Myricetin	12 ± 1	>20
Quercetin	16 ± 1	>20
Genistein	16 ± 2	>20
[NSAIDs]		
Ibuprofen	1.2 ± 0.1	>20
Flufenamic acid	2.2 ± 0.1	>20
Loxoprofen	9.9 ± 1.2	>20
Indomethacin	20 ± 1	15 ± 2
Zomepirac	>20	2.3 ± 0.1
Other drugs[c]	>20	>20
[Fatty acids]		
Arachidonic acid ($20{:}4^{cis-5,8,11,14}$)	0.76 ± 0.12	2.1 ± 0.2
Linoleic acid ($18{:}2^{cis-9,12}$)	1.3 ± 0.1	2.2 ± 0.1
Oleic acid ($18{:}1^{cis-9}$)	3.9 ± 0.4	2.1 ± 0.1
Palmitoleic acid ($16{:}1^{cis-9}$)	6.2 ± 0.2	5.3 ± 0.1
Fatty acid derivatives[d]	>20	>20

[a] Structures of hexestrol, flavonoids and NSAIDs are shown in Supplementary Fig. S4, and those of fatty acids are indicated in parentheses that show their numbers of carbon atoms and double bonds followed by configuration and location of the double bonds.

[b] >20, less than 35% inhibition at 20 μM.

[c] NSAIDs (ketoprofen, sulindac, fenoprofen and flurbiprofen) and other drugs (medroxyprogesterone acetate, glycyrrhetinic acid, ethacrynic acid and furosemide).

[d] Elaidic acid ($18{:}1^{trans-9}$), methyl linoleate, oleyl alcohol and linoleyl alcohol.

3.3. Tissue expression of R1C19 and 20HSDL

In the NCBI gene database, the mRNA for R1C19 is noted to be ubiquitously expressed in both sexes of Fischer 344 rats across four developmental stages (2-, 6-, 21-, and 104-weeks-old), in contrast to restricted expression of 20HSDL mRNA in the adult kidney, liver and testis [35]. We analyzed the expressions of the two enzymes in tissues of adult Wistar rats by RT-PCR (Fig. 3). The transcript of R1C19 was detected in all the tissues, in which the adrenal gland and colon showed the low expression. In contrast, 20HSDL showed biased expression: Its intense signal was observed in the kidney, and weaker bands were detected in the liver, testis, brain, heart and colon. Thus, there is no significant difference in tissue expression of the two enzymes between the two rat strains.

3.4. Possible roles of R1C19 and 20HSDL in PG metabolism

9α-Hydroxy-PGs were endogenous substrates of both R1C19 and 20HSDL, of which 20HSDL was more efficient and exhibited the highest k_{cat}/K_m value for 13,14-dihydro-15-keto-$PGF_{2\alpha}$. The substrate specificity is suggested that the two enzymes act as NAD^+-dependent 9HPDs. Previously, high NAD^+-dependent 9HPD activity using 13,14-dihydro-15-keto-$PGF_{2\alpha}$ as the substrate was detected in the cytosol of adult rat kidney homogenate [36–39], although the activity was low in other rat tissues such as liver, testis and lung [38]. In addition, NAD^+-dependent 9HPD activity towards PGI_2 (or its hydrolyzed form, 6-keto-$PGF_{1\alpha}$) was reported to be expressed in rat kidney and platelets [40,41]. Since the substrate specificity and inhibitor sensitivity of the enzymes are different, 9HPD has been suggested to exist in two or more isoforms in rat tissues [42]. Despite of these studies using rat tissue cytosols, only one 9HPD was purified from rat kidney cytosol [30]. This 9HPD is a 33-kDa monomer catalyzing the 4-pro-*R* (A-specific) hydrogen transfer from the PG substrate to NAD^+, and oxidizes 13, 14-dihydro-15-keto-$PGF_{2\alpha}$, 15-keto-$PGF_{2\alpha}$ and PGF_2, but not 6-keto-$PGF_{1\alpha}$ that is formed by spontaneous hydrolysis of PGI_2. However, the cDNA or gene for the purified 9HPD has been identified yet.

Most members of the AKR superfamily are about 37-kDa monomers showing NAD(P)H-based 4-pro-*R* hydrogen transfer [1,2], which are similar to those of 9HPD purified from rat kidney [30]. Several members of the AKR1C subfamily also show oxidoreductase activity towards PGs [2,11,43]. In rat AKR1Cs, NADP(H)-preferring AKR1C9 exhibits low 9-, 11- and 15-hydroxy-PG dehydrogenase activity using $NADP^+$ as the coenzyme [34]. Among the NAD^+-preferring rat AKRs (1C16, 1C17 and

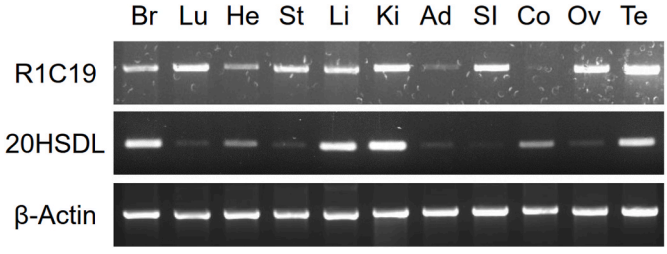

Fig. 3. RT-PCR analysis for expression of mRNAs for R1C19 and 20HSDL in rat tissues. Tissues: brain (Br), lung (Lu), heart (He), stomach (St), liver (Li), kidney (Ki), adrenal gland (Ad), small intestine (SI), colon (Co), ovary (Ov) and testis (Te). The expression of mRNA for β-actin is shown as the control.

1C24, Table 1), AKR1C24 was reported to oxidize $PGF_{2\alpha}$ and 9α,11β-PGF_2 at low rates [15]. When the PG specificity of the rat NAD^+-preferring AKR1Cs was analyzed, AKR1C24 and AKR1C16, but not AKR1C17, oxidized 13,14-dihydro-15-keto-$PGF_{2\alpha}$ and PGD_2 (Table 5) with low V_{max}/K_m values. Among the examined AKR1Cs, 20HSDL is the most efficient 9HPD, and its kinetic constants for 13,14-dihydro-15-keto-$PGF_{2\alpha}$, 15-keto-$PGF_{2\alpha}$ and $PGF_{2\alpha}$ are comparable to those of rat kidney 9HPD [30], suggesting that 20HSDL is identical to rat kidney 9HPD. This is also supported by following properties: 1) Like rat kidney 9HPD [30], 20HSDL did not oxidize PGI_2, and showed low reaction reversibility and high coenzyme preference for NAD^+. 2) Inhibitor sensitivity to flavonoid naringenin [40], drugs (indomethacin, furosemide and ethacrynic acid) [30,38] and *cis*-unsaturated fatty acids [30] of rat kidney 9HPD is similar to that of 20HSDL (Table 4). 3) The high expression of the mRNA for 20HSDL in the kidney is in agreement with the early reports of 9HPD activities in rat tissues [36–39]. Only one difference between 20HSDL and rat kidney 9HPD is that PGD_2, a substrate of 20HSDL, was previously reported to be a weak inhibitor of rat kidney 9HPD [30]. The activity of rat kidney 9HPD was determined by measuring the transfer of tritium from 13,14-dihydro-15-keto-[9β-^{3}H]$PGF_{2\alpha}$ to lactate by coupling with lactate dehydrogenase. In such assay method, the addition of another substrate, PGD_2, results in competition with the radioactive 13,14-dihydro-15-keto-$PGF_{2\alpha}$ for binding to the enzyme. The mixed substrate phenomenon causes decrease in oxidation rate of the radioactive 13,14-dihydro-15-keto-$PGF_{2\alpha}$, which may be judged to inhibition by PGD_2 in the previous study [30]. Thus, 20HSDL functions as a major form of 9HPD in rat kidney, whereas the other NAD^+-preferring rat AKRs (R1C19, AKR1C16 [13] and AKR1C24 [15]) are ubiquitously distributed, and may act as other 9HPD isoforms that were previously suggested [39,40,42].

The possible PG metabolism proceeded by the presently characterized enzymes is illustrated in Fig. 4. 9HPD is reported to be responsible to the metabolism of $PGF_{2\alpha}$ to 13,14-dihydro-15-keto-PGE_2 [30,36–39]. Rat 9HPD isoforms suggested [42] probably result from four NAD^+-preferring AKR1Cs (20HSDL, R1C19, AKR1C24 and AKR1C16). In addition, the present study suggests that these enzymes are involved in the metabolism of PGD_2. In rat tissues, PGD_2 is formed by PGD synthases and/or via the isoprostane pathway [44–46] and is metabolized to 9α,11β-PGF_2 by PGD_2 11-ketoreductase [47,48]. The four NAD^+-preferring AKR1Cs oxidize PGD_2 to PGK_2, which is speculated from their substrate specificity for 9α-hydroxy-PGs. Similarly to the case with 20HSDL (Fig. 2), PGK_2 was not detected in the product analysis of PGD_2 oxidation by R1C19, AKR1C24 and AKR1C16 (data not shown). In addition, PGK_2 is currently not detected in animal tissues. This might be due to instability of PGK_2 in aqueous solution, although the reason for its instability must be revealed by further study. 9α,11β-PGF_2 was oxidized by 20HSDL, R1C19 and AKR1C24, and its oxidized product was 11β-PGE_2, which is detected in rodent tissues [46,49], inhibits PGE_2 binding to rat hypothalamic membranes [50] and stimulates rat bone resorption [51]. However, the metabolic pathway to form 11β-PGE_2 has not been reported. The present study suggests a novel biosynthetic pathway of 11β-PGE_2 by 9HPD activity of the AKR1Cs at least in rat tissues.

In the NCBI gene database (https://www.ncbi.nlm.nih.gov/gene), genes that encode proteins with >86% ASI to 20HSDL are annotated in five rodents (Supplementary Table S2), but such a gene does not exist in the genome of mouse (*Mus musculus*). In contrast, genes (encoding proteins with >87% ASI to R1C19) are annotated in many rodents including mouse, whose ortholog is AKR1C19 as shown in Tables 1 and S2. Like R1C19, AKR1C19 is expressed in many mouse tissues, and shows the substrate specificity for xenobiotic alcohols and α-dicarbonyl compounds, but its endogenous substrates are unknown [14]. Therefore, we examined whether mouse AKR1C19 oxidizes the newly found R1C19 substrates (hydroxysteroids, PGs and β-ionol) in the presence of NAD^+. As shown in Table 6, mouse AKR1C19 also oxidized these substrates with kinetic constants similar to those of R1C19. Although its role in the steroid metabolism is obscure because of the existence of AKR1C12 and AKR1C13 showing more efficient 17β-HSD activity [12,13], AKR1C19 may also be involved in the metabolism of 9-hydroxy-PGs in mouse tissues, in which 20HSDL-like 9HPD and its gene have not been reported.

4. Conclusions

This study shows that R1C19 and 20HSDL encoded in rat *akr1c19* and *RGD1564865* genes exhibit NAD^+-linked dehydrogenase activity towards 9α-hydroxy-PGs ($PGF_{2\alpha}$ series, PGD_2 and 9α,11β-PGF_2). In addition, it was found that other NAD^+-preferring AKR1Cs (1C16 and 1C24) oxidize the 9α-hydroxy-PGs. Among the enzymes, 20HSDL is catalytically most efficient and abundantly expressed in rat kidney, in contrast to ubiquitous distribution of the other enzymes in rat tissues. 20HSDL also differs from R1C19, AKR1C16 and AKR1C24 in its insensitivity to inhibitors (hexestrol and flavonoids). The comparison of enzymic features of the four enzymes with PG dehydrogenases suggests not only the identity of 20HSDL and a major form of 9HPD in rat kidney [30], but also a relationship of R1C19 and other AKR1Cs with 9HPD isoforms in non-renal tissues. Furthermore, this study suggests novel metabolic pathways for PGD_2 and 9α,11β-PGF_2 to their 9-keto metabolites.

Table 5
Comparison of PG specificity among rat kidney 9HPD and NAD^+-preferring AKR1Cs.

Substrate	Parameter[a]	9HPD[b]	20HSDL	R1C19	AKR1C24	AKR1C16
13,14-Dihydro-15-keto-$PGF_{2\alpha}$	K_m	0.33	0.31 ± 0.05	35 ± 3	120 ± 19	9.7 ± 0.3
	V_{max}	9.12	21 ± 2	41 ± 6	77 ± 8	4.1 ± 0.1
	V_{max}/K_m	28	69	1.2	0.64	0.42
15-Keto-$PGF_{2\alpha}$	K_m	3.0	2.6 ± 0.2	18 ± 1	83 ± 14	22 ± 3
	V_{max}	5.84	25 ± 1.5	10 ± 1	1.6 ± 0.2	2.9 ± 0.2
	V_{max}/K_m	1.9	9.6	0.56	0.019	0.13
PGD_2	K_m		1.8 ± 0.2	12 ± 1	23 ± 3	21 ± 3
	V_{max}	nr	39 ± 4	2.2 ± 0.3	9.6 ± 4	14 ± 1
	V_{max}/K_m		22	0.18	0.42	0.67
9α,11β-PGF_2	K_m		14 ± 2	264 ± 25	24[c]	
	V_{max}	nr	29 ± 4	4.4 ± 0.8	4.0[c]	ns[d]
	V_{max}/K_m		1.7	0.017	0.17[c]	
$PGF_{2\alpha}$	K_m	5.0	9.2 ± 0.6	215 ± 15	72[c]	
	V_{max}	1.37	15 ± 0.9	3.5 ± 0.5	4.6[c]	ns[d]
	V_{max}/K_m	0.27	1.6	0.017	0.065[c]	

[a] Units of K_m and V_{max} are μM and nmol of formed NADH/min/mg of enzyme, respectively.
[b] The values are taken from Ref. [30]. nr, not reported.
[c] The values are taken from Ref. [15].
[d] ns, no significant activity was observed.

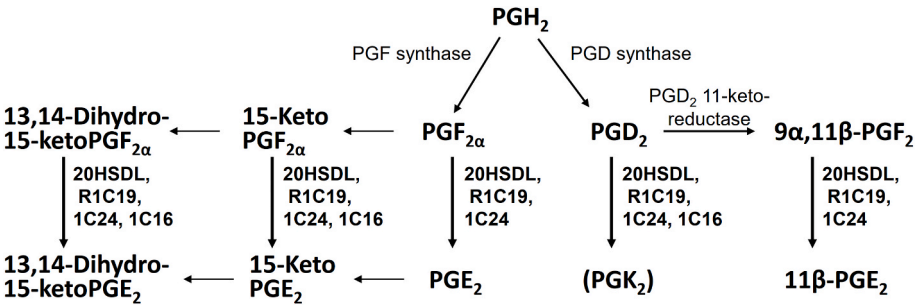

Fig. 4. Possible PG metabolism proceeded by rat 20HSDL, R1C19 and AKR1Cs (1C16 and 1C24).

Table 6
Substrate specificity for β-ionol, hydroxysteroids and PGs of mouse AKR1C19.

Substrate	K_m (μM)	k_{cat} (min^{-1})	k_{cat}/K_m (min^{-1} mM^{-1})
β-Ionol	10 ± 1	0.74 ± 0.11	11
5β-Androstane-3α,17β-diol	14 ± 3	0.21 ± 0.02	15
5β-Androstan-17β-ol-3-one	82 ± 7	0.41 ± 0.07	5.0
Testosterone	220 ± 33	0.34 ± 0.03	1.5
13,14-Dihydro-15-keto-$PGF_{2\alpha}$	118 ± 14	4.2 ± 0.3	36
15-Keto-$PGF_{2\alpha}$	41 ± 4	1.4 ± 0.1	34
PGD_2	27 ± 3	0.26 ± 0.01	9.6
9α,11β-PGF_2	510 ± 61	0.41 ± 0.07	0.80
$PGF_{2\alpha}$	270 ± 38	0.17 ± 0.01	0.63

Acknowledgements

The DNA sequence analysis was performed in the Division of Genomic Research in Life Science Research Center, Gifu University.

Appendix A. Supplementary data

Supplementary data related to this article can be found at https://doi.org/10.1016/j.abb.2021.108755.

References

[1] T.M. Penning, The aldo-keto reductases (AKRs): Overview, Chem. Biol. Interact. 234 (2015) 236–246, https://doi.org/10.1016/j.cbi.2014.09.024.
[2] T.M. Penning, P. Wangtrakuldee, R.J. Auchus, Structural and functional biology of aldo-keto reductase steroid-transforming enzymes, Endocr. Rev. 40 (2019) 447–475, https://doi.org/10.1210/er.2018-00089.
[3] T.L. Rižner, T.M. Penning, Role of aldo-keto reductase family 1 (AKR1) enzymes in human steroid metabolism, Steroids 79 (2014) 49–63. https://doi: 10.1016/j.steroids.2013.10.012.T.
[4] T. Matsunaga, S. Shintani, A. Hara, Multiplicity of mammalian reductases for xenobiotic carbonyl compounds, Drug Metabol. Pharmacokinet. 21 (2006) 1–18, https://doi.org/10.2133/dmpk.21.1.
[5] Y. Deyashiki, K. Ohshima, M. Nakanishi, et al., Molecular cloning and characterization of mouse estradiol 17β-dehydrogenase (A-specific), a member of the aldo-keto reductase family, J. Biol. Chem. 270 (1995) 10461–10467, https://doi.org/10.1074/jbc.270.18.10461.
[6] A. Hara, Y. Inoue, M. Nakagawa, et al., Purification and characterization of NADP$^+$-dependent 3α-hydroxysteroid dehydrogenase from mouse liver cytosol, J. Biochem. 103 (1988) 1027–1034, https://doi.org/10.1093/oxfordjournals.jbchem.a122374.
[7] V. Bellemare, F. Labrie, V. Luu-The, Isolation and characterization of a cDNA encoding mouse 3α-hydroxysteroid dehydrogenase: an androgen-inactivating enzyme selectively expressed in female tissues, J. Steroid Biochem. Mol. Biol. 98 (2006) 18–24, https://doi.org/10.1016/j.jsbmb.2005.07.004.
[8] S. Ishikura, S. Nakajima, T. Kaneko, et al., Comparison of stereoselective reduction of 3- and 20-oxosteroids among mouse and primate 20α-hydroxysteroid dehydrogenases, in: H. Weiner, B. Plapp, R. Lindahl, E. Maser (Eds.), Enzymology and Molecular Biology of Carbonyl Metabolism 12, Purdue University Press, West Lafayette, 2005, pp. 341–351.
[9] S. Ishikura, N. Usami, S. Nakajima, et al., Characterization of two isoforms of mouse 3(17)α-hydroxysteroid dehydrogenases of the aldo-keto reductase family, Biol. Pharm. Bull. 27 (2004) 1939–1945, https://doi.org/10.1248/bpb.27.1939.
[10] K. Matsumoto, S. Endo, S. Ishikura, et al., Enzymatic properties of a member (AKR1C20) of the aldo-keto reductase family, Biol. Pharm. Bull. 29 (2006) 539–542, https://doi.org/10.1248/bpb.29.539.
[11] S. Endo, T. Matsunaga, A. Hara, Mouse Akr1cl gene product is a prostaglandin D_2 11-ketoreductase with strict substrate specificity, Arch. Biochem. Biophys. 674 (2019) 108096, https://doi.org/10.1016/j.abb.2019.108096.
[12] S. Endo, K. Matsumoto, T. Matsunaga, et al., Substrate specificity of a mouse aldo-keto reductase (AKR1C12), Biol. Pharm. Bull. 29 (2006) 2488–2492, https://doi.org/10.1248/bpb.29.2488.
[13] S. Endo, M. Sanai, K. Horie, et al., Characterization of rat and mouse NAD$^+$-dependent 3α/17β/20α-hydroxysteroid dehydrogenases and identification of substrate specificity determinants by site-directed mutagenesis, Arch. Biochem. Biophys. 467 (2007) 76–86, https://doi.org/10.1016/j.abb.2007.08.011.
[14] S. Ishikura, K. Horie, M. Sanai, et al., Enzymatic properties of a member (AKR1C19) of the aldo-keto reductase family, Biol. Pharm. Bull. 28 (2005) 1075–1078, https://doi.org/10.1248/bpb.28.1075.
[15] S. Ishikura, K. Matsumoto, M. Sanai, K. Horie, et al., Molecular cloning of a novel type of rat cytoplasmic 17β-hydroxysteroid dehydrogenase distinct from the type 5 isozyme, J. Biochem. 139 (2006) 1053–1063, https://doi.org/10.1093/jb/mvj109.
[16] T.M. Penning, Y. Jin, V.V. Heredia, M. Lewis, Structure-function relationships in 3α-hydroxysteroid dehydrogenases: a comparison of the rat and human isoforms, J. Steroid Biochem. Mol. Biol. 85 (2003) 247–255, https://doi.org/10.1016/s0960-0760(03)00236-x.
[17] T.M. Penning, I. Mukharji, S. Barrows, P. Talalay, Purification and properties of a 3α-hydroxysteroid dehydrogenase of rat liver cytosol and its inhibition by anti-inflammatory drugs, Biochem. J. 222 (1984) 601–611, https://doi.org/10.1042/bj2220601.
[18] H. Ma, T.M. Penning, Characterization of homogeneous recombinant rat ovarian 20α-hydroxysteroid dehydrogenase: fluorescent properties and inhibition profile, Biochem. J. 341 (1999) 853–859.
[19] S. Endo, T. Matsunaga, K. Horie, et al., Enzymatic characteristics of an aldo-keto reductase family protein (AKR1C15) and its localization in rat tissues, Arch. Biochem. Biophys. 465 (2007) 136–147, https://doi.org/10.1016/j.abb.2007.05.008.
[20] M. Sanai, S. Endo, T. Matsunaga, et al., Rat NAD$^+$-dependent 3α-hydroxysteroid dehydrogenase (AKR1C17): a member of the aldo-keto reductase family highly expressed in kidney cytosol, Arch. Biochem. Biophys. 464 (2007) 122–129, https://doi.org/10.1016/j.abb.2007.04.003.
[21] C.C. O'Meara, M. Hoffman, W.E. Sweeney Jr., et al., Role of genetic modifiers in an orthologous rat model of ARPKD, Physiol. Genom. 44 (2012) 741–753, https://doi.org/10.1152/physiolgenomics.00187.2011.
[22] B.B. Roques, J. Leghait, M.Z. Lacroix, et al., The nuclear receptors pregnane X receptor and constitutive androstane receptor contribute to the impact of fipronil on hepatic gene expression linked to thyroid hormone metabolism, Biochem. Pharmacol. 86 (2013) 997–1039, https://doi.org/10.1016/j.bcp.2013.08.012.
[23] K. Platt, F. Oesch, An improved synthesis of trans-5,6-dihydroxy-1,3-cyclohexadiene (*trans*-1,2-dihydroxy-1,2-dihydrobenzene), Synthesis 7 (1977) 449–450.
[24] J. Sambrook, E.F. Fritsch, T. Maniatis, Molecular Cloning: A Laboratory Manual, second ed., Cold Spring Harbor Laboratory Press, New York, 1989.
[25] M.M. Bradford, A rapid and sensitive method for the quantitation of microgram quantities of protein utilizing the principle of protein-dye binding, Anal. Biochem. 72 (1976) 248–254, https://doi.org/10.1006/abio.1976.9999.

[26] N. Iwata, N. Inazu, T. Satoh, The purification and properties of NADPH-dependent carbonyl reductases from rat ovary, J. Biochem. 105 (1989) 556–564, https://doi.org/10.1093/oxfordjournals.jbchem.a122704.
[27] T. Ohta, S. Ishikura, S. Shintani, et al., Kinetic alteration of a human dihydrodiol/3α-hydroxysteroid dehydrogenase isoenzyme, AKR1C4, by replacement of histidine-216 with tyrosine or phenylalanine, Biochem. J. 352 (2000) 685–691, https://doi.org/10.1042/bj3520685.
[28] R.L. Veech, L.V. Eggleston, H.A. Krebs, The redox state of free nicotinamide-adenine dinucleotide phosphate in the cytoplasm of rat liver, Biochem. J. 115 (1969) 609–619, https://doi.org/10.1042/bj1150609a.
[29] H. Shimada, K. Miura, Y. Imamura, Characteristics and inhibition by flavonoids of 20α-hydroxysteroid dehydrogenase activity in mouse tissues, Life Sci. 78 (2006) 2931–2936, https://doi.org/10.1016/j.lfs.2005.11.022.
[30] B. Yuan, C.L. Tai, H.H. Tai, 9-Hydroxyprostaglandin dehydrogenase from rat kidney. Purification to homogeneity and partial characterization, J. Biol. Chem. 255 (1980) 7439–7443.
[31] H. Osama, S. Narumiya, O. Hayaishi, et al., Inhibition of brain prostaglandin D synthetase and prostaglandin D_2 dehydrogenase by some saturated and unsaturated fatty acids, Biochim. Biophys. Acta 752 (1983) 251–258.
[32] A. Hara, S. Endo, T. Matsunaga, et al., Long-chain fatty acids inhibit human members of the aldo-keto reductase 1C subfamily, J. Biochem. 162 (2017) 371–379, https://doi.org/10.1093/jb/mvx041.
[33] A. Hara, S. Endo, T. Matsunaga, et al., Human carbonyl reductase 1 participating in intestinal first-pass drug metabolism is inhibited by fatty acids and acyl-CoAs, Biochem. Pharmacol. 138 (2017) 185–192, https://doi.org/10.1016/j.bcp.2017.04.023.
[34] T.M. Penning, R.B. Sharp, Prostaglandin dehydrogenase activity of purified rat liver 3α-hydroxysteroid dehydrogenase, Biochem. Biophys. Res. Commun. 148 (1987) 646–652, https://doi.org/10.1016/0006-291x(87)90925-9.
[35] Y. Yu, J.C. Fuscoe, C. Zhao, et al., A rat RNA-Seq transcriptomic BodyMap across 11 organs and 4 developmental stages, Nat. Commun. 5 (2014) 3230, https://doi.org/10.1038/ncomms4230.
[36] C. Pace-Asciak, Prostaglandin 9-hydroxydehydrogenase activity in the adult rat kidney. Identification, assay, pathway, and some enzyme properties, J. Biol. Chem. 250 (1975) 2789–2794.
[37] C.P. Asciak, Z. Domazet, 9-Hydroxyprostaglandin dehydrogenase activity in the adult rat kidney. Regional distribution and sub-fractionation, Biochim. Biophys. Acta 380 (1975) 338–343, https://doi.org/10.1016/0005-2760(75)90019-3.
[38] H.H. Tai, B. Yuan, A simple and sensitive assay for 9-hydroxyprostaglandin dehydrogenase, Anal. Biochem. 78 (1977) 410–422, https://doi.org/10.1016/0003-2697(77)90102-6.
[39] P.K. Moore, R.J. Griffiths, F.J. Lofts, The effect of some flavone drugs on the conversion of prostacyclin to 6-oxoprostaglandin E_1, Biochem. Pharmacol. 32 (1983) 2813–2817, https://doi.org/10.1016/0006-2952(83)90097-7.
[40] R.J. Griffiths, P.K. Moore, Conversion of prostacyclin to 6-oxo-prostaglandin E_1 by rat, rabbit, Guinea-pig and human platelets, Br. J. Pharmacol. 80 (1983) 395–402, https://doi.org/10.1111/j.1476-5381.1983.tb10046.x.
[41] C.R. Pace-Asciak, Z. Domazet, 9-Hydroxyprostaglandin dehydrogenase in rat kidney cortex converts prostaglandin I_2 into 15-keto-13,14-dihydro 6-ketoprostaglandin E_1, Biochim. Biophys. Acta 796 (1984) 129–135, https://doi.org/10.1016/0005-2760(84)90339-4.
[42] R.J. Griffiths, C.N. Berry, J.R. Hoult, P.K. Moore, Age-dependent changes in the synthesis and catabolism of 6-oxo-PGE_1 and other prostanoids by the rat kidney in vitro, Biochem. Pharmacol. 34 (1985) 223–228, https://doi.org/10.1016/0006-2952(85)90128-5.
[43] K. Watanabe, Recent reports about enzymes related to the synthesis of prostaglandin (PG) F_2 ($PGF_{2\alpha}$ and 9α,11β-PGF_2), J. Biochem. 150 (2011) 593–596, https://doi.org/10.1093/jb/mvr116.
[44] M. Ujihara, Y. Urade, N. Eguchi N, et al., Prostaglandin D_2 formation and characterization of its synthetases in various tissues of adult rats, Arch. Biochem. Biophys. 260 (1988) 521–531, https://doi.org/10.1016/0003-9861(88)90477-8.
[45] M.C. Fernández-Tomé, C. D'Antuono, V.L. Kahane, et al., Compartmental study of rat renal prostaglandin synthesis during development, Biol. Neonate 70 (1996) 235–245, https://doi.org/10.1159/000244370.
[46] L. Gao, W.E. Zackert, J.J. Hasford, et al., Formation of prostaglandins E_2 and D_2 via the isoprostane pathway: a mechanism for the generation of bioactive prostaglandins independent of cyclooxygenase, J. Biol. Chem. 278 (2003) 28479–28489, https://doi.org/10.1074/jbc.M303984200.
[47] H. Hayashi, S. Ito, K. Watanabe, et al., Metabolism of prostaglandin D_2 in isolated rat lung: the stereospecific formation of 9α,11β-prostaglandin F_2 from prostaglandin D_2, Biochim. Biophys. Acta 917 (1987) 356–364.
[48] J.R. Hoult, K.B. Bacon, D.J. Osborne, C. Robinson, Organ selective conversion of prostaglandin D_2 to 9α,11β-prostaglandin F_2 and its subsequent metabolism in rat, rabbit and Guinea pig, Biochem. Pharmacol. 37 (1988) 3591–3599, https://doi.org/10.1016/0006-2952(88)90389-9.
[49] S.A. Brose, B.T. Thuen, M.Y. Golovko, LC/MS/MS method for analysis of E_2 series prostaglandins and isoprostanes, J. Lipid Res. 52 (2011) 850–859, https://doi.org/10.1194/jlr.D013441.
[50] F. Dray, M. Heaulme, Prostaglandins of the E series inhibit release of noradrenaline in rat hypothalamus by a mechanism unrelated to classical alpha 2 adrenergic presynaptic inhibition, Neuropharmacology 23 (1984) 457–462, https://doi.org/10.1016/0028-3908(84)90255-7.
[51] L.G. Raisz, F.N. Woodiel, Effect of alterations in the cyclopentane ring on bone resorptive activity of prostaglandin, Prostaglandins 37 (1989) 229–235, https://doi.org/10.1016/0090-6980(89)90059-2.